

Parton transverse momenta and Drell-Yan dilepton production

A. Szczurek^{1,2,*} and G. Ślipek^{1,†}

¹*Institute of Nuclear Physics PAN, PL-31-342 Cracow, Poland*

²*University of Rzeszów, PL-35-959 Rzeszów, Poland*

(Dated: October 27, 2018)

Abstract

The differential cross section for the dilepton production is calculated including Fermi motion of hadron constituents as well as emission from the ladders in the formalism of unintegrated parton distributions. We use unintegrated parton distributions which fulfil Kwieciński evolution equations. Both zeroth- and first-order (for matrix element) contributions are included. We calculate azimuthal angular correlations between charged leptons and deviations from the $p_t(l^+) = p_t(l^-)$ relation. We concentrate on the distribution in dilepton-pair transverse momentum. We find incident energy and virtuality dependence of the distribution in transverse momentum of the lepton pair. We study also azimuthal correlations between jet and dilepton pair and correlation in the $(p_{1t}(jet), p_{2t}(l^+l^-))$ space. The results are compared with experimental data of the R209 and UA1 collaborations.

PACS numbers: 12.38.Bx, 12.38.Cy

*Electronic address: Antoni.Szczurek@ifj.edu.pl

†Electronic address: Gabriela.Slipek@ifj.edu.pl

I. INTRODUCTION

The Drell-Yan dilepton production is one of representative examples for which QCD collinear perturbative calculation can be performed order-by-order. Usually inclusive distributions are discussed. The most often studied observables are: $d\sigma/dM_{ee}$ or $d\sigma/dx_F$, where M_{ee} is invariant mass of the dilepton pair and x_F is the Feynman variable of the pair. In this paper we concentrate rather on one- and two-dimensional distributions which are singular in the standard collinear approximation.

In the 0-th order collinear approximation (quark-antiquark annihilation) the transverse momentum of the dilepton pair (sum of transverse momenta of opposite sign charged leptons) is zero due to momentum conservation. Then the 0th-order result is not included in calculating the distribution in dilepton transverse momentum. The lowest nonzero contributions are 1-st order quark-antiquark annihilation and QCD Compton. Typical for collinear approach they show singularity at small dilepton transverse momentum.

Due to inter-quark interactions the quarks/antiquarks, constituents of hadrons, are not at rest and possess nonzero transverse momenta. Already this effect causes that the 0-th order process contributes to the finite transverse momenta of the lepton pair. Furthermore the emissions of gluons before the $q\bar{q} \rightarrow l^+l^-$ hard process causes an extra k_t -smearing which, via momentum conservation, lead to finite transverse momenta of the dilepton pair (see Fig.1). The initial transverse momenta are often modelled effectively in terms of phenomenological Gaussian distributions [1, 2]. The effect of Fermi motion as well as emission from the ladders can be easily included in the formalism of Kwiecinski unintegrated parton distributions [3].

In the present paper we wish to calculate differential cross section for dilepton production in the formalism of unintegrated parton distributions. We shall include both 0-th order and 1-st order contributions. We shall concentrate on the distributions in dilepton transverse momentum. This observable is extremely sensitive in the 0-th order to the initial transverse momenta of partons. The transverse momentum of Drell-Yan pair was calculated within next-to-leading order perturbative QCD [4] as well as in the resummation formalism in the impact parameter space [5]. Our approach differs in details from those approaches.

Our results will be compared with experimental data for elementary proton-proton or proton-antiproton scattering. We leave analysis of proton-nucleus scattering for a separate publication.

II. FORMALISM

A. 0-th order Drell-Yan cross section

The differential cross section for the 0-th order contribution can be written as:

$$\begin{aligned} \frac{d\sigma}{dy_1 dy_2 d^2p_{1t} d^2p_{2t}} = \sum_f \int \frac{d^2\kappa_{1t}}{\pi} \frac{d^2\kappa_{2t}}{\pi} \frac{1}{16\pi^2(x_1 x_2 s)^2} \\ \delta^2(\vec{\kappa}_{1t} + \vec{\kappa}_{2t} - \vec{p}_{1t} - \vec{p}_{2t}) [\mathcal{F}_{q_f}(x_1, \kappa_{1t}^2, \mu_F^2) \mathcal{F}_{\bar{q}_f}(x_2, \kappa_{2t}^2, \mu_F^2) \overline{|M(q\bar{q} \rightarrow e^+e^-)|^2} \\ + \mathcal{F}_{\bar{q}_f}(x_1, \kappa_{1t}^2, \mu_F^2) \mathcal{F}_{q_f}(x_2, \kappa_{2t}^2, \mu_F^2) \overline{|M(q\bar{q} \rightarrow e^+e^-)|^2}] , \end{aligned} \quad (2.1)$$

where $\mathcal{F}_i(x_1, \kappa_{1t}^2)$ and $\mathcal{F}_i(x_2, \kappa_{2t}^2)$ are unintegrated quark/antiquark distributions in hadron h_1 and h_2 , respectively.

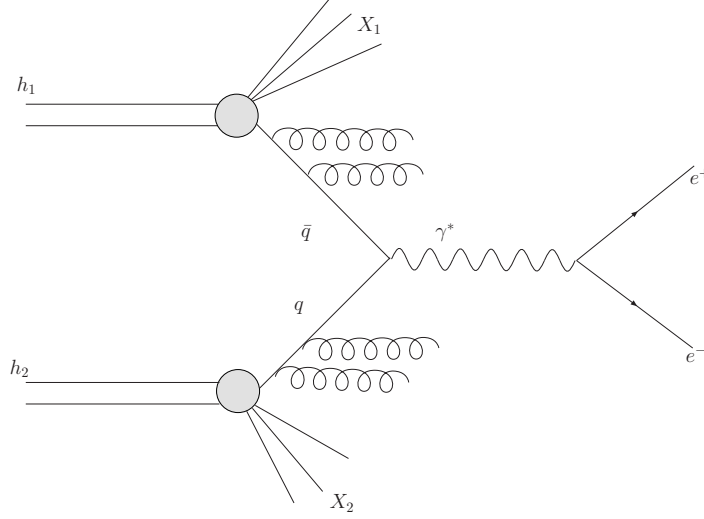


FIG. 1: The diagram for the 0-th order Drell-Yan dilepton production with initial emissions from the ladders.

The longitudinal momentum fractions are evaluated in terms of final lepton rapidities and transverse momenta:

$$\begin{aligned} x_1 &= \frac{m_{1t}}{\sqrt{s}} \exp(y_1) + \frac{m_{2t}}{\sqrt{s}} \exp(y_2) , \\ x_2 &= \frac{m_{1t}}{\sqrt{s}} \exp(-y_1) + \frac{m_{2t}}{\sqrt{s}} \exp(-y_2), \end{aligned} \quad (2.2)$$

where $m_t = \sqrt{p_t^2 + m^2}$ is a so-called transverse mass.

The delta function in Eq.(2.1) can be eliminated as e.g. in Refs.[6, 7, 8].

Formally, if the following replacements

$$\begin{aligned} \mathcal{F}_i(x_1, \kappa_{1t}^2, \mu_F^2) &\rightarrow x_1 p_i(x_1, \mu_F^2) \delta(\kappa_{1t}^2) , \\ \mathcal{F}_j(x_2, \kappa_{2t}^2, \mu_F^2) &\rightarrow x_2 p_j(x_2, \mu_F^2) \delta(\kappa_{2t}^2) \end{aligned} \quad (2.3)$$

are done one recovers standard text book formulae.

B. 1-st order Drell-Yan cross section

In the first order in α_s there are two types of diagrams: QCD Compton and quark-antiquark annihilation. A typical diagrams for corresponding subprocesses are shown in Fig.2.

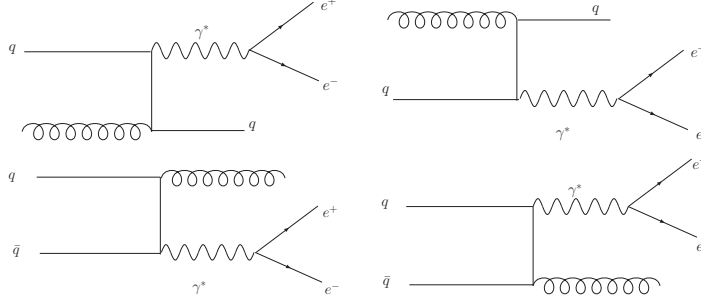


FIG. 2: The subprocess diagrams for the 1-st order Drell-Yan dilepton production with initial emissions from the ladders.

For example the multi-differential cross section for the QCD Compton can be written in terms of unintegrated quark/antiquark and gluon distributions as:

$$\frac{d\sigma(h_1 h_2 \rightarrow \gamma^* X)}{dy_1 dy_2 d^2 p_{1t} d^2 p_{2t}} = \sum_f \int \frac{d^2 \kappa_{1t}}{\pi} \frac{d^2 \kappa_{2t}}{\pi} \frac{1}{16\pi^2 (x_1 x_2 s)^2} \delta^2(\vec{\kappa}_{1t} + \vec{\kappa}_{2t} - \vec{p}_{1t} - \vec{p}_{2t}) [\mathcal{F}_g(x_1, \kappa_{1t}^2, \mu_F^2) \mathcal{F}_{q_f}(x_2, \kappa_{2t}^2, \mu_F^2) \overline{|M(gq \rightarrow \gamma^* q)|^2} + \mathcal{F}_{q_f}(x_1, \kappa_{1t}^2, \mu_F^2) \mathcal{F}_g(x_2, \kappa_{2t}^2, \mu_F^2) \overline{|M(qg \rightarrow \gamma^* q)|^2}] . \quad (2.4)$$

Similarly the cross section for the first-order quark-antiquark annihilation associated with gluon emission can be written as

$$\frac{d\sigma(h_1 h_2 \rightarrow \gamma^* X)}{dy_1 dy_2 d^2 p_{1t} d^2 p_{2t}} = \sum_f \int \frac{d^2 \kappa_{1t}}{\pi} \frac{d^2 \kappa_{2t}}{\pi} \frac{1}{16\pi^2 (x_1 x_2 s)^2} \delta^2(\vec{\kappa}_{1t} + \vec{\kappa}_{2t} - \vec{p}_{1t} - \vec{p}_{2t}) [\mathcal{F}_{\bar{q}_f}(x_1, \kappa_{1t}^2, \mu_F^2) \mathcal{F}_{q_f}(x_2, \kappa_{2t}^2, \mu_F^2) \overline{|M(\bar{q}q \rightarrow \gamma^* g)|^2} + \mathcal{F}_{q_f}(x_1, \kappa_{1t}^2, \mu_F^2) \mathcal{F}_{\bar{q}_f}(x_2, \kappa_{2t}^2, \mu_F^2) \overline{|M(q\bar{q} \rightarrow \gamma^* g)|^2}] . \quad (2.5)$$

The delta functions in Eq.(2.4) and Eq.(2.5) can be eliminated as e.g. in Refs.[6, 7, 8].

The cross section for the emission of the dilepton pair can be expressed in terms of the cross section for the emission of time-like photon written above times a probability of the transition of the virtual photon into dilepton pair as:

$$\frac{d\sigma(h_1 h_2 \rightarrow l^+ l^- j X)}{dM_{ll}^2} = \frac{\alpha_{em}}{3\pi M_{ll}^2} d\sigma(h_1 h_2 \rightarrow \gamma^* j X) , \quad (2.6)$$

where M_{ll} is the dilepton invariant mass. Please note that $M_{ll}^2 = Q^2$, where Q^2 is virtuality of the time-like photon.

C. Nonperturbative region of small M_{ll}

The formalism presented up to here applies in the perturbative region when the dilepton invariant mass M_{ll} is not too small. How to calculate Drell-Yan production for small invariant masses ($M_{ll} < 1$ GeV) is not completely clear and this issue was not discussed in the literature. In the region of very small photon virtualities the standard formulae presented

in the section above do not apply directly and some modifications are necessary (the same is true for soft-gluon resummation method). The reason is twofold. First of all the parton distribution may not exist for very small scales. Secondly, there is a singularity when photon virtuality approaches 0.

In the present analysis we shall use the following extrapolation procedure:

Firstly, to be able to use the perturbative Kwieciński parton distributions the factorization scale for UPDFs is taken as:

$$\mu_F^2 = M_{ll}^2 + Q_s^2, \quad (2.7)$$

instead of $\mu_F^2 = M_{ll}^2$ used usually in calculating Drell-Yan cross section for large dilepton invariant masses.

Secondly, to avoid singularities inherent in the matrix element ($\hat{s} \rightarrow 0$) we use a simple replacement proposed in Ref.[2, 9]:

$$\begin{aligned} \hat{s} &\rightarrow \hat{s} + Q_s^2, \\ \hat{t} &\rightarrow \hat{t} - Q_s^2/2, \\ \hat{u} &\rightarrow \hat{u} - Q_s^2/2. \end{aligned} \quad (2.8)$$

The parameter Q_s^2 is to be adjusted to experimental data. The above procedure allows to avoid singularity when $M_{ll} \rightarrow 0$. Please note that such a replacement does not change $\hat{s} + \hat{t} + \hat{u}$.

The procedure described above is very similar in spirit to that used in calculating the "deep inelastic" structure function F_2 for small photon virtualities [10, 11].

For illustration in Fig.3 we present distributions in transverse momentum of one of the leptons: electron or positron (left panel) and distributions in transverse momentum of the pair of leptons (right panel) for different values of the parameter Q_s^2 . In this calculation we have used unintegrated parton distributions to be discussed in the next subsection. The results depend somewhat on the value of the parameter. In principle, the shift parameter Q_s^2 could be adjusted to experimental data for extremely low dilepton invariant masses. It is not clear a priori if such a procedure can be successful.

D. Unintegrated parton distributions

Due to its simplicity the Gaussian smearing of initial transverse momenta is a good reference for other approaches. It allows to study phenomenologically the role of transverse momenta in several high-energy processes. We define a simple unintegrated parton distributions:

$$\mathcal{F}_i^{Gauss}(x, \kappa^2, \mu_F^2) = x p_i^{coll}(x, \mu_F^2) \cdot f_{Gauss}(\kappa^2), \quad (2.9)$$

where $p_i^{coll}(x, \mu_F^2)$ are standard collinear (integrated) parton distribution ($i = g, q, \bar{q}$) and $f_{Gauss}(\kappa^2)$ is a Gaussian two-dimensional function:

$$f_{Gauss}(\kappa^2) = \frac{1}{2\pi\sigma_0^2} \exp(-\kappa_t^2/2\sigma_0^2) / \pi. \quad (2.10)$$

The UPDFs defined by Eq.(2.9) and (2.10) is normalized such that:

$$\int \mathcal{F}_i^{Gauss}(x, \kappa^2, \mu_F^2) d\kappa^2 = x p_i^{coll}(x, \mu_F^2). \quad (2.11)$$

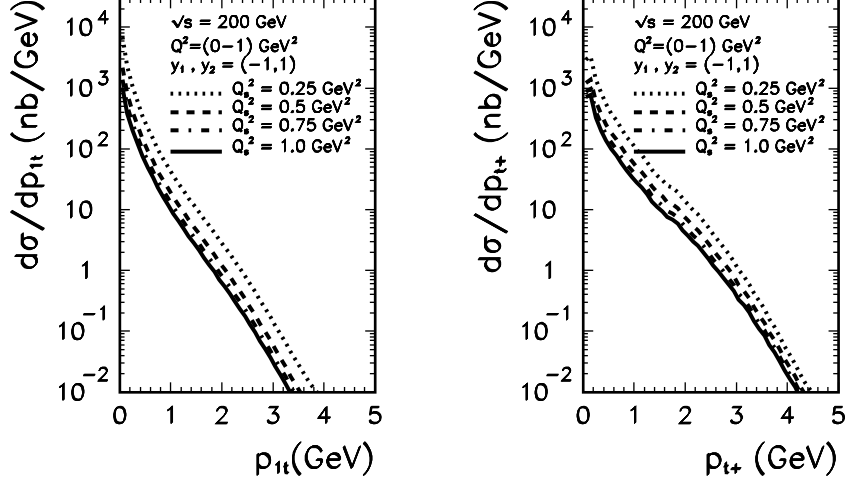


FIG. 3: Distributions in transverse momentum of the electron or positron (left panel) and in the transverse momentum of the pair (right panel) in the nonperturbative region of $Q^2 \in (0,1)$ GeV^2 at $W = 200$ GeV and for different values of the parameter Q_s^2 . In this calculation $Q_s^2 = 0.25$ (dotted), 0.5 (dashed), 0.75 (dash-dotted), 1.0 (solid) GeV^2 (from top to bottom). Here midrapidity electrons and positrons $y_1, y_2 \in (-1,1)$ were selected for illustration.

Kwieciński has shown that the evolution equations for unintegrated parton distributions takes a particularly simple form in the variable conjugated to the parton transverse momentum. In the impact-parameter space the Kwieciński equation takes the following simple form

$$\begin{aligned}
\frac{\partial \tilde{f}_{NS}(x, b, \mu^2)}{\partial \mu^2} &= \frac{\alpha_s(\mu^2)}{2\pi\mu^2} \int_0^1 dz P_{qq}(z) \left[\Theta(z-x) J_0((1-z)\mu b) \tilde{f}_{NS}\left(\frac{x}{z}, b, \mu^2\right) \right. \\
&\quad \left. - \tilde{f}_{NS}(x, b, \mu^2) \right], \\
\frac{\partial \tilde{f}_S(x, b, \mu^2)}{\partial \mu^2} &= \frac{\alpha_s(\mu^2)}{2\pi\mu^2} \int_0^1 dz \left\{ \Theta(z-x) J_0((1-z)\mu b) \left[P_{qq}(z) \tilde{f}_S\left(\frac{x}{z}, b, \mu^2\right) \right. \right. \\
&\quad \left. \left. + P_{qg}(z) \tilde{f}_G\left(\frac{x}{z}, b, \mu^2\right) \right] - [zP_{qq}(z) + zP_{gq}(z)] \tilde{f}_S(x, b, \mu^2) \right\}, \\
\frac{\partial \tilde{f}_G(x, b, \mu^2)}{\partial \mu^2} &= \frac{\alpha_s(\mu^2)}{2\pi\mu^2} \int_0^1 dz \left\{ \Theta(z-x) J_0((1-z)\mu b) \left[P_{gq}(z) \tilde{f}_S\left(\frac{x}{z}, b, \mu^2\right) \right. \right. \\
&\quad \left. \left. + P_{gg}(z) \tilde{f}_G\left(\frac{x}{z}, b, \mu^2\right) \right] - [zP_{gg}(z) + zP_{qg}(z)] \tilde{f}_G(x, b, \mu^2) \right\}.
\end{aligned} \tag{2.12}$$

We have introduced here the short-hand notation

$$\begin{aligned}
\tilde{f}_{NS} &= \tilde{f}_u - \tilde{f}_{\bar{u}}, \quad \tilde{f}_d - \tilde{f}_{\bar{d}}, \\
\tilde{f}_S &= \tilde{f}_u + \tilde{f}_{\bar{u}} + \tilde{f}_d + \tilde{f}_{\bar{d}} + \tilde{f}_s + \tilde{f}_{\bar{s}}.
\end{aligned} \tag{2.13}$$

The unintegrated parton distributions in the impact factor representation are related to the familiar collinear distributions as follows

$$\tilde{f}_k(x, b=0, \mu^2) = \frac{x}{2} p_k(x, \mu^2) . \quad (2.14)$$

On the other hand, the transverse momentum dependent UPDFs are related to the integrated parton distributions as

$$xp_k(x, \mu^2) = \int_0^\infty d\kappa_t^2 \mathcal{F}_k(x, \kappa_t^2, \mu^2) . \quad (2.15)$$

The two possible representations are interrelated via Fourier-Bessel transform

$$\begin{aligned} \mathcal{F}_k(x, \kappa_t^2, \mu^2) &= \int_0^\infty db \, b J_0(\kappa_t b) \tilde{f}_k(x, b, \mu^2) , \\ \tilde{f}_k(x, b, \mu^2) &= \int_0^\infty d\kappa_t \, \kappa_t J_0(\kappa_t b) \mathcal{F}_k(x, \kappa_t^2, \mu^2) . \end{aligned} \quad (2.16)$$

The index k above numerates either gluons ($k=0$), quarks ($k>0$) or antiquarks ($k<0$).

While physically $\mathcal{F}_k(x, \kappa_t^2, \mu^2)$ should be positive, there is no obvious reason for such a limitation for $\tilde{f}_k(x, b, \mu^2)$.

In the following we use leading-order parton distributions from Ref.[12] as the initial condition for QCD evolution. The set of integro-differential equations in b -space was solved by the method based on the discretisation made with the help of the Chebyshev polynomials (see [3]). Then the unintegrated parton distributions were put on a grid in x , b and μ^2 and the grid was used in practical applications for Chebyshev interpolation.

For the calculation of inclusive and coincidence cross section for the heavy (time-like) photon production (see next section) the parton distributions in momentum space are more useful. These calculation requires a time-consuming multi-dimensional integration. An explicit calculation of the Kwieciński UPDFs via Fourier transform for needed in the main calculation values of (x_1, κ_{1t}^2) and (x_2, κ_{2t}^2) is not possible. Therefore it becomes a necessity to prepare auxiliary grids of the momentum-representation UPDFs before the actual calculation of the cross sections. These grids are then used via a two-dimensional interpolation in the spaces (x_1, κ_{1t}^2) and (x_2, κ_{2t}^2) associated with each of the two incoming partons.

III. A COMMENT ON b -SPACE RESUMMATION

There is an alternative approach to calculate transverse momentum distribution of the dilepton pair. In the Collins-Soper-Sterman formalism [13] (see also[5]), known also as b -space resummation, the cross section differential in dilepton invariant mass (M_{ll}), rapidity of the pair (y) and transverse momentum of the pair (p_{t+}) can be written as

$$\frac{d\sigma}{dM_{ll}^2 dy dp_{t+}^2} = \frac{1}{(2\pi)^2} \int d^2b \exp(i\vec{p}_t \vec{b}) W(b, M_{ll}, x_1, x_2) = \frac{1}{2\pi} \int db b J_0(p_{t+} b) W(b, M_{ll}, x_1, x_2) . \quad (3.1)$$

The integrand function $W(b, M_{ll}^2, p_{t+}, x_1, x_2)$ for the Drell-Yan pair production is:

$$\begin{aligned}
W(b, M_{ll}^2, p_{t+}, x_1, x_2) = & \frac{4\pi^2\alpha^2}{9M_{ll}^2s} \sum_f e_f^2 e^{-S(b, M_{ll}^2)} \\
& \left(\sum_a \int_{x_1}^1 \frac{d\xi_1}{\xi_1} f_{a/h_1} \left(\xi_1, \frac{1}{b^2} \right) C_{fa} \left(\frac{x_1}{\xi_1}; b \right) \right) \\
& \left(\sum_b \int_{x_2}^1 \frac{d\xi_2}{\xi_2} f_{b/h_2} \left(\xi_2, \frac{1}{b^2} \right) C_{fb} \left(\frac{x_2}{\xi_2}; b \right) \right) \\
& + \frac{4\pi^2\alpha^2}{9M_{ll}^2s} Y(M_{ll}^2, p_{t+}, x_1, x_2) .
\end{aligned} \tag{3.2}$$

The first term is naturally called resummation term and the function Y gives a correction which is negligible for small p_{t+} . The decomposition (3.2) is not free of ambiguities, like matching condition etc. Furthermore it is not easy to assure that in each corner of the phase space (y, M_{ll}, p_{t+}) the resummation part of the cross section is positive. For $p_{t+} \ll M_{ll}$ the resummation term is much bigger than the correction term. The formula (3.1) together with (3.2) has a singularity when $M_{ll} \rightarrow 0$ due to the photon propagator. In Eq.(3.2) the exponent in the Sudakov-like form factors reads

$$S(b, Q^2) = \int_{\mu_{min}^2(b)}^{Q^2} \frac{d\mu^2}{\mu^2} \left[\log \left(\frac{Q^2}{\mu^2} \right) A(\alpha_s(\mu^2)) + B(\alpha_s(\mu^2)) \right] . \tag{3.3}$$

The coefficients A and B can be expanded in the series of α_s [13].

In this approach longitudinal momentum fractions are calculated as a rule as for the collinear 0th-order kinematics:

$$\begin{aligned}
x_1 &= \exp(+y) \frac{M_{ll}}{\sqrt{s}}, \\
x_2 &= \exp(-y) \frac{M_{ll}}{\sqrt{s}} .
\end{aligned} \tag{3.4}$$

Please note that this is slightly different than in our case, where the transverse momenta of leptons explicitly enter into corresponding formulae. The soft-gluon resummation formula could be corrected for finite p_{t+} .

The coefficient functions C_{fi} can be expanded in terms of α_s

$$\begin{aligned}
C_{fa} &= \delta_{fa} \delta(1 - \xi_1) + \dots , \\
C_{fb} &= \delta_{fb} \delta(1 - \xi_2) + \dots ,
\end{aligned} \tag{3.5}$$

where the dots represent higher order terms in α_s . Limiting to the resummation term in (3.2) and keeping only first terms in the expansion (a bit academic approximation used here for simplicity) one gets

$$\begin{aligned}
W^{res}(b, M_{ll}^2, p_t, x_1, x_2) \approx & \frac{4\pi^2\alpha^2}{9M_{ll}^2s} \sum_f e_f^2 e^{-S(b, M_{ll}^2)} \\
& \left[q_f \left(x_1, \frac{1}{b^2} \right) \bar{q}_f \left(x_2, \frac{1}{b^2} \right) + \bar{q}_f \left(x_1, \frac{1}{b^2} \right) q_f \left(x_2, \frac{1}{b^2} \right) \right] .
\end{aligned} \tag{3.6}$$

Obviously $b \ll 1/\Lambda$ in order that the pQCD is at work. The region of large b is of nonperturbative nature. In order to supplement to the whole b space an extrapolation is needed. Usually this is done with the help of the following prescription:

$$b \rightarrow b_* = \frac{b}{(1 + b^2/b_{max}^2)^{1/2}} < b. \quad (3.7)$$

Above b_{max} is a free, a bit arbitrary parameter ($1/b_{max}^2 > \mu_0^2$, where μ_0^2 is a minimal possible factorization scale). To cut off contributions of large impact factor an extra form factor $F^{NP}(b, x_1, x_2, \dots)$ multiplying $W^{res}(b, M_{ll}, p_{t+}, x_1, x_2)$ is introduced. Above dots represent a set of free parameters. These parameters must be found by fitting to experimental data. Typical, not small, uncertainties are shown e.g. in Fig.1 of Ref.[5] (see also [15]).

Our approach here was formulated in the momentum space. Let us limit (as in the b -space resummation) to distributions in y , p_{t+} and M_{ll}^2 . Then the cross section can be written approximately(!) as

$$\begin{aligned} \frac{d\sigma}{dy d^2 p_{t+} dM_{ll}^2} \approx \sum_f \frac{\sigma_f^{DY}}{s x_1 x_2} \int \frac{d^2 k_{1t}}{\pi} \frac{d^2 k_{2t}}{\pi} \\ (f_{q_f}(x_1, k_{1t}^2, \mu_F^2) f_{\bar{q}_f}(x_2, k_{2t}^2, \mu_F^2) + f_{\bar{q}_f}(x_1, k_{1t}^2, \mu_F^2) f_{q_f}(x_2, k_{2t}^2, \mu_F^2)) \delta^2(\vec{k}_{1t} + \vec{k}_{2t} - \vec{p}_{t+}), \end{aligned} \quad (3.8)$$

where $\sigma_f^{DY} = \frac{1}{3} e_f^2 \frac{4\pi\alpha^2}{3s}$. Analogously as for the W and Z boson production (see Ref.[16]) the spectrum in y , p_{t+} and M_{ll}^2 can be written also in terms of b -space unintegrated parton distributions. The corresponding cross section then reads:

$$\begin{aligned} \frac{d\sigma}{dy d^2 p_{t+} dM_{ll}^2} = \frac{4\pi\alpha^2}{9M_{ll}^2 \hat{s}} \frac{1}{\pi^2} \sum_f e_f^2 \int d^2 b J_0(p_{t+} b) \\ \left[\tilde{f}_{q/1}(x_1, b, \mu_F^2) \tilde{f}_{\bar{q}/2}(x_2, b, \mu_F^2) + \tilde{f}_{\bar{q}/1}(x_1, b, \mu_F^2) \tilde{f}_{q/2}(x_2, b, \mu_F^2) \right]. \end{aligned} \quad (3.9)$$

In most of the evaluations presented in this paper $\mu_F^2 = M_{ll}^2$ is used.

We wish to note very similar structure of the b -space resummation formula (3.1) with (3.6) and our formula (3.9). Assuming a factorizable form for the nonperturbative form factor¹:

$$F_{q\bar{q}}^{NP}(Q, b, x_1, x_2) = F_q^{NP}(Q, b, x_1) \cdot F_{\bar{q}}^{NP}(Q, b, x_2) \quad (3.10)$$

one could define b -space resummation unintegrated (anti)quark distributions in the b -space as:

$$\begin{aligned} f_{q_f}^{SGR}(x_1, b, Q^2) = F_q(b, x_1, Q^2) [x_1 q_f(x_1, \mu^2(b)) + \dots] \exp\left(-\frac{1}{2} S(b, Q^2)\right), \\ f_{\bar{q}_f}^{SGR}(x_2, b, Q^2) = F_{\bar{q}}(b, x_2, Q^2) [x_2 \bar{q}_f(x_2, \mu^2(b)) + \dots] \exp\left(-\frac{1}{2} S(b, Q^2)\right). \end{aligned} \quad (3.11)$$

¹ This is justified if the main nonperturbative effects are due to the merging of initial (anti)quarks in bound (nonperturbative) hadrons which causes that initial partons are not at rest and posses internal momenta.

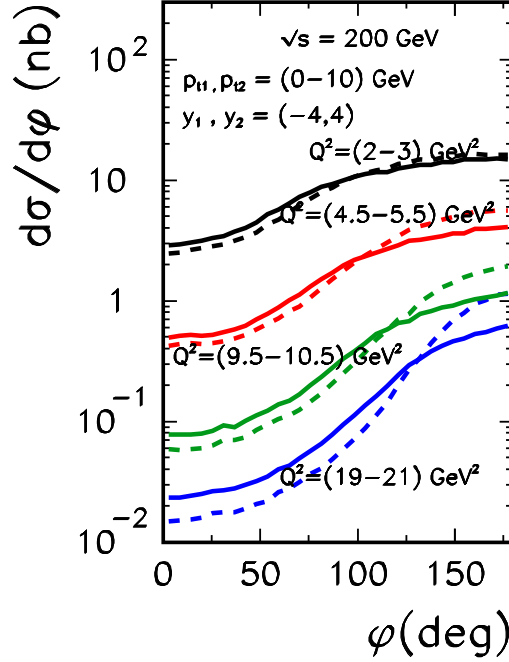


FIG. 4: Distributions in azimuthal angle between electron and positron in proton-proton scattering for RHIC energy $\sqrt{s} = 200$ GeV and different windows in Q^2 specified in the figure. The dashed lines are for UPDFs with Gaussian smearing ($\sigma_0 = \frac{\sqrt{2}}{2} \frac{1}{b_0}$, $b_0 = 1 \text{ GeV}^{-1}$) and the solid lines are for Kwieciński UPDFs with $b_0 = 1 \text{ GeV}^{-1}$. Here $\mu_F^2 = Q^2$ was chosen. No cuts on lepton transverse momenta were applied.

The b -space resummation is useful for calculating transverse momentum distribution of the dilepton pair, a variable Fourier-conjugated to b . For other correlation observables between e^+ and e^- exact kinematics and new kinematical variables must be used. This seems not possible in the framework of the b -space resummation. Our approach, formulated in the momentum space and with explicit kinematics of each lepton, is better suited for calculating observables like $\frac{d\sigma}{d\phi_{ee}}$ or $\frac{d\sigma}{dp_{t,e^+} dp_{t,e^-}}$ discussed in the present paper.

IV. RESULTS

A. 0-th order component with transverse momenta

In the standard collinear approach in 0-th order approximation leptons of opposite charge are produced back-to-back, i.e. the relative azimuthal angle between them is fixed and equals to 180° . The situation changes if one includes "initial" transverse momenta of partons which annihilate producing dilepton pair. This is shown in Fig.4.

We have selected RHIC energy ($\sqrt{s} = 200$ GeV) for illustration. Since the plot is purely theoretical we did not make any cuts on electron/positron transverse momenta and rapidi-

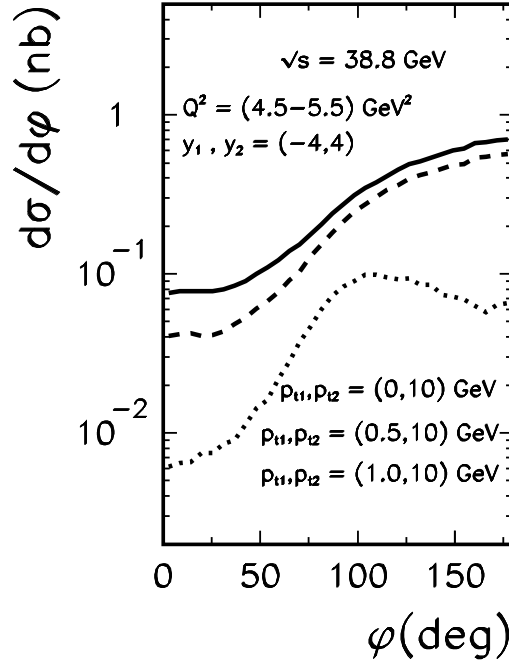


FIG. 5: The influence of cuts on lepton transverse momenta on distributions in azimuthal angle between electron and positron for $\sqrt{s} = 38.8$ GeV (E772 experiment). Here $\mu_F^2 = Q^2$ was chosen.

ties. We show results for narrow bins in photon virtuality (= square of the dilepton invariant mass) specified in the figure. Of course, the cross section strongly depends on photon virtuality; the smaller virtuality the bigger cross section. This is mainly a kinematical effect. This can be seen by comparison of solid (Kwieciński UPDFs) and dashed (Gaussian smearing) lines. In this calculation σ_0 of the Gaussian distribution was adjusted to b_0 in the Kwieciński UPDFs. For small virtualities the two distributions almost coincide. At large virtuality they differ much more which can be understood as effect of evolution of UPDFs from the initial scale μ_0^2 to Q^2 .

How the azimuthal angle correlations depend on cuts in lepton transverse momenta? In Fig.5 we show some examples for the E772 experiment at Fermilab. The cuts not only lower the cross section but also modify the shape of azimuthal correlations.

In collinear 0th-order approximation the electron and positron transverse momenta compensate each other, i.e. $p_{1t}(e^+) = p_{2t}(e^-)$. In the k_t -factorization approach this condition is relaxed. As an example in Fig.6 we show two dimensional maps in the region of relatively small transverse momenta ($p_{1t}, p_{2t} < 5$ GeV). In this calculation we did not put any constraint on photon virtuality (dilepton invariant mass). In the left panel we show results obtained with Eq.(2.1). As discussed in the theoretical section real perturbative calculation requires presence of large scales. Therefore to be precise the perturbative calculation at small transverse momenta is not reliable. This can be better understood by looking at Fig.7 which shows correlations of transverse momenta and photon virtualities. In the right panel of Fig.6 we show in addition calculation with shifted scales and kinematical variables.

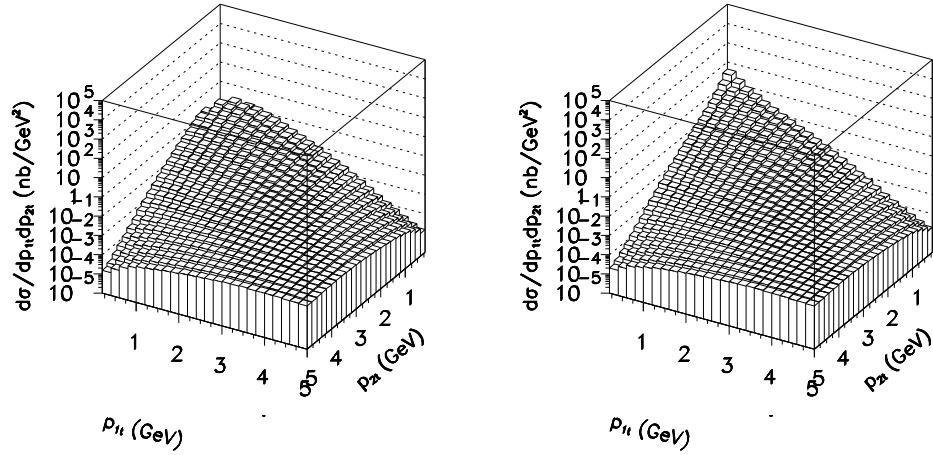


FIG. 6: Distribution in $(p_{1t}(e^+), p_{2t}(e^-))$ for zeroth-order Drell-Yan in proton-proton collisions at $\sqrt{s} = 200$ GeV. In the left panel standard procedure is used with $\mu_F^2 = Q^2$ and in the right panel in addition $Q_s^2 = 1$ GeV² is used as described in subsection IIC. In this calculation $-1 < y_1, y_2 < 1$.

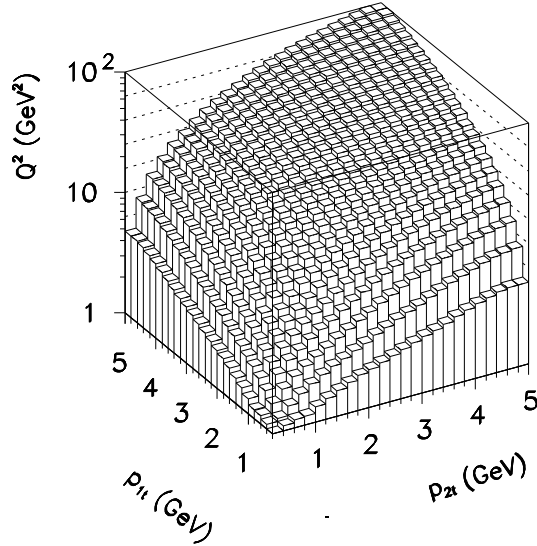


FIG. 7: Average value of the photon virtuality on the $(p_{1t}(e^+), p_{2t}(e^-))$ plane for zeroth-order Drell-Yan in proton-proton collisions at $\sqrt{s} = 200$ GeV. Here $\mu_F^2 = Q^2$ and $-1 < y_1, y_2 < 1$.

A careful inspection of both panels shows that the differences are only at small transverse momenta. A more orthodox approach would be to completely exclude the region of small transverse momenta of leptons, which means also small dilepton invariant masses.

Very interesting observable, which is singular in collinear approximation in leading-order, is the distribution in the transverse momentum of the dilepton pair (p_{t+}) . In Fig.8 we show such a dependence on the incident center-of-mass energy for two different bins in photon

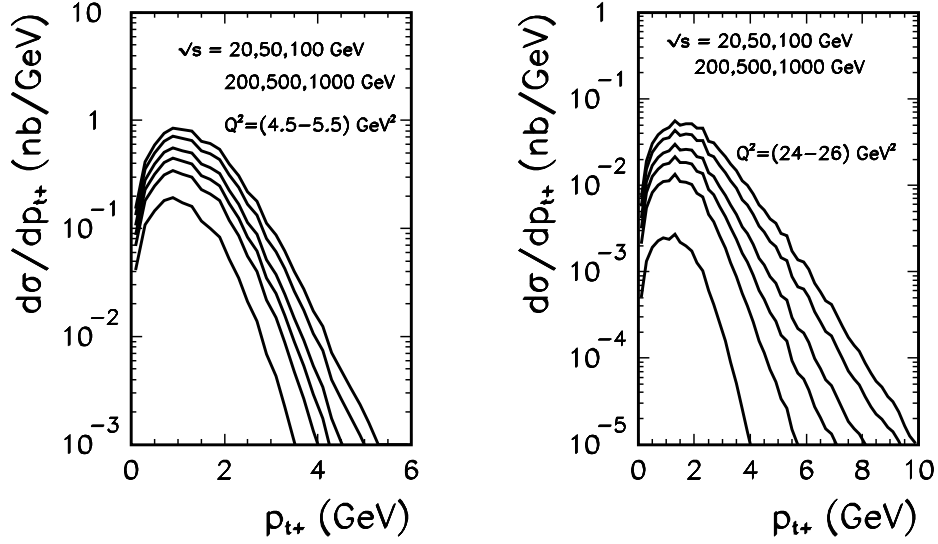


FIG. 8: Distribution in p_{t+} for different beam energies specified in the figure and for two different windows in Q^2 . Here $\mu_F^2 = Q^2$.

virtuality. In general, the bigger energy the broader the distribution in p_{t+} ². The bigger energies correspond to smaller values of quark/antiquark longitudinal momentum fractions. The effect of broadening of the distribution is larger for larger photon-virtuality which is taken as a factorization scale in the Kwieciński UPDFs.

The effect of broadening is summarized in Fig.9 where is show average value of the lepton-pair transverse momentum. The difference between different bins in photon virtuality is due to QCD evolution effect (we use photon virtuality Q^2 as a factorization scale in the Kwieciński unintegrated parton distributions). Similar effects were already discussed for dijet [7] and photon-jet correlations [8]. The two curves in Fig.9 would coincide if the evolution effect would be neglected, as was done e.g. in Ref.[2].

We show the effect of broadening also for the RHIC energy $\sqrt{s} = 200$ GeV where we show distribution in p_{t+} for different bins in photon virtuality. The effect of broadening is inherently related to the Kwieciński UPDFs where the initial k_{1t}^2 and/or k_{2t}^2 smearing depends on the factorization scale and on x_1 and/or x_2 (see discussion in [3, 7, 8]).

Finally we wish to confront our calculation with existing data for the Drell-Yan dilepton production. In Fig.10 we show our results with different values of the parameter b_0 in the Kwieciński UPDFs [3]. The parameter b_0 quantifies nonperturbative effects which are beyond evolution effects embodied in the Kwieciński evolution equations. The dominant effect is probably the Fermi motion of nucleon constituents. This effect is often neglected in the standard QCD calculations. We get quite good description of the R209 collaboration data already in the zeroth-order with $b_0 = 1 - 2$ GeV⁻¹. This is a bit surprising, as the zeroth-order contribution is usually neglected in orthodox collinear approach. It seems therefore

² In collinear approach the distribution would be delta function in transverse momentum of the pair.

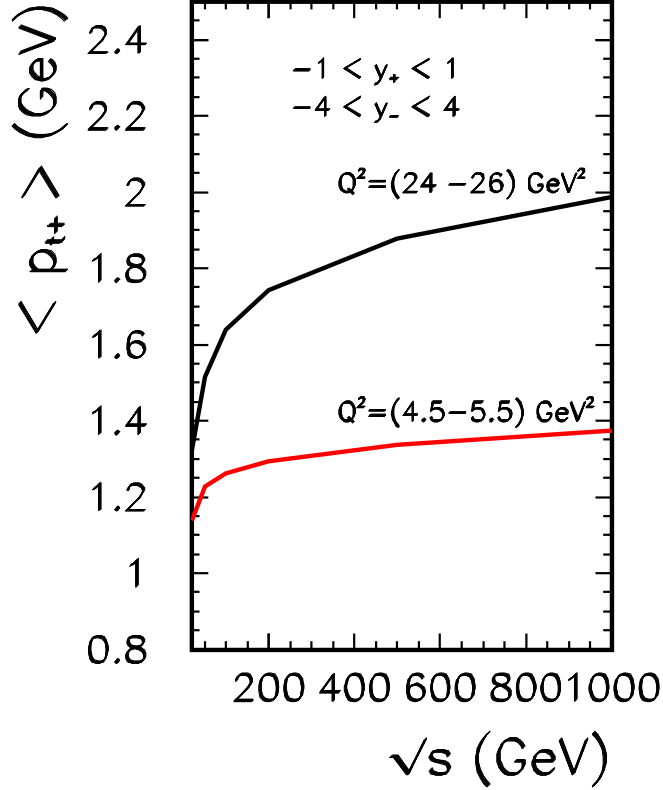


FIG. 9: Average value of p_{t+} as a function of center-of-mass energy for two different windows of Q^2 . Here $\mu_F^2 = Q^2$.

indispensable to include higher-orders in the k_t -factorization approach. We shall discuss this issue in the next section.

B. 1-st order component with transverse momenta

Let us now discuss contribution of processes of one order higher than in the previous section, with hard subprocesses shown in Fig.2. These diagrams have to be inserted between two partonic ladders.

The correlation in azimuthal angle between jet and the dilepton pair is shown in Fig.11. One can see a strong deviation from the collinear back-to-back kinematics caused by the transverse momenta of initial partons. The most top (thick) lines are for the full phase space. The intermediate lines are with extra cuts on e^+e^- and jet rapidities. The most bottom lines are for extra cuts on transverse momenta of the associated jet $p_t(jet) > 5$ GeV. The latter cut changes drastically the shape of distributions which are peaked now more at $\phi = 180^\circ$.

In Fig.12 we show corresponding transverse momentum distribution of the dilepton pair

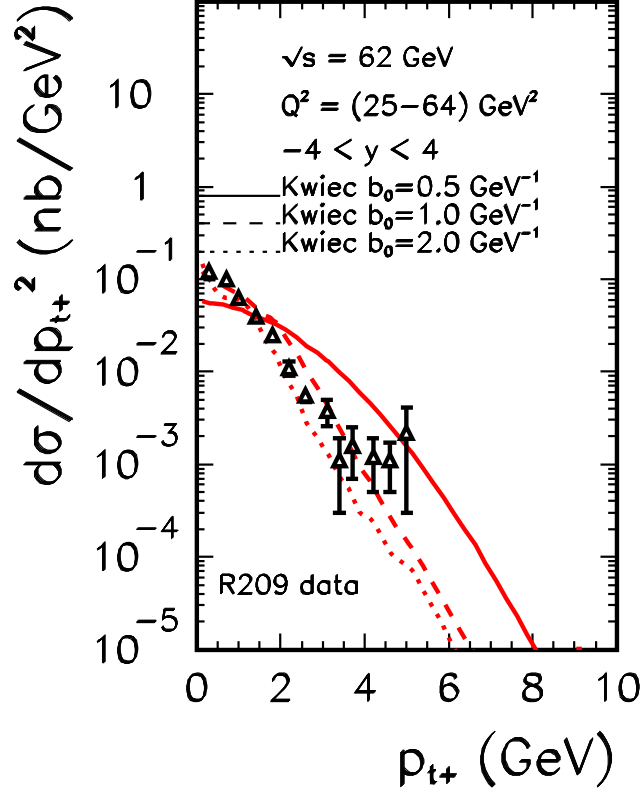


FIG. 10: Distribution in p_{t+} for zero-order Drell-Yan in proton-proton collisions for $\sqrt{s} = 62$ GeV. Different curves correspond to different values of the b_0 parameter in the Kwieciński UPDFs. The experimental data of the R209 collaboration are taken from [17].

for RHIC energy $\sqrt{s} = 200$ GeV. For comparison we show also zeroth-order contribution discussed in the previous section. The zeroth-order contribution dominates at small transverse momenta, while the first-order contribution at transverse momenta larger than about 5 GeV. Here we include both Compton and annihilation processes. The first-order contributions have no singularity at $p_t(e^+e^-)$ as in the collinear approach. The zeroth and first-order contributions overlap only in a very limited range of $p_t(e^+e^-) \approx 4$ GeV. The zeroth-order k_t -factorization component includes some higher order contributions via UPDFs. However, because the two contributions occupy rather different parts of the phase space no severe double counting is expected.

When integrated the first-order contribution is significantly smaller than the zeroth-order one. This can be better seen in Fig.13 where we show rapidity distributions. We show the zeroth-order (LO) and two k_t -factorization Compton components: QCD Compton ($qg \rightarrow qe^+e^-$ and $gq \rightarrow qe^+e^-$) and quark-antiquark annihilation ($q\bar{q} \rightarrow ge^+e^-$ and $\bar{q}q \rightarrow ge^+e^-$).

Let us present now the first-order contributions together with existing data. In Fig.14 we present separately two first-order contributions: Compton and quark-antiquark annihilation. The sum of the both contributions is shown by the thin solid line. This contribution is

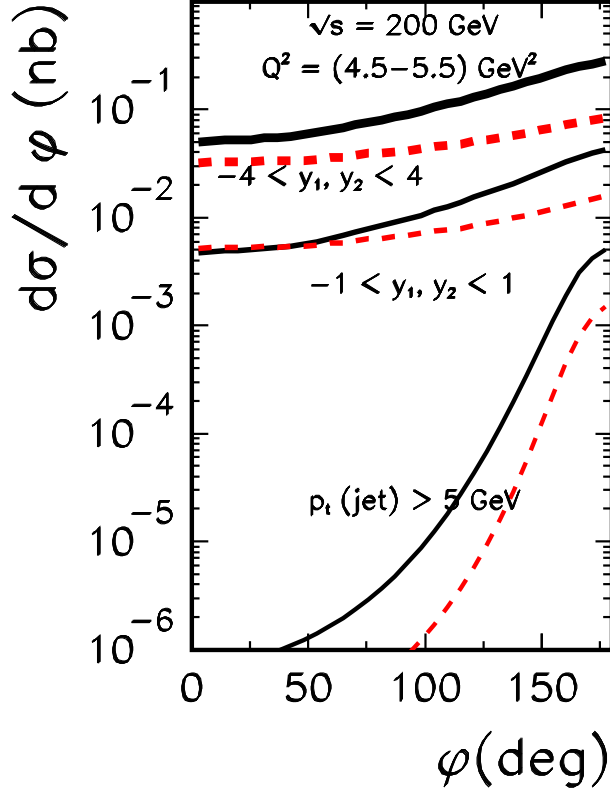


FIG. 11: Distribution in azimuthal angle between jet and dilepton pair in proton-proton collisions for the RHIC energy $\sqrt{s} = 200$ GeV for the QCD Compton (solid lines) and quark-antiquark annihilation (dashed lines). The results for $-1 < y(e^+e^-), y(jet) < 1$ are shown with thin lines and the results for $-4 < y(e^+e^-), y(jet) < 4$ are shown with thick lines.

about factor of 4 smaller than the R209 collaboration data. For comparison we show also the zeroth-order contribution. The 0th-order contribution is much larger than the 1st-order one. The situation may change at larger transverse momenta. The sum of the 0th- and 1st-order well describe the transverse momentum data. The scenario discussed here seems quite different than the one presented in the text book by Field [19] where the data were described by a convolution of the collinear first-order component and some extra, somewhat arbitrary, Gaussian smearing and where the zeroth-order contribution was completely ignored.

In Fig.15 we compare distributions obtained in collinear and k_t -factorization approach. The difference can be seen in small transverse momentum region. Above $p_{t+} > 4$ GeV the two approaches practically give the same results. The singularities seen for collinear approximation disappear when transverse momenta of initial partons are included.

The first-order contribution becomes dominant at larger transverse momenta of the dilepton pairs. This is shown in Fig.16 where we present transverse momentum distribution of dimuons of opposite charge for proton-antiproton scattering at the center-of-mass energy $\sqrt{s} = 630$ GeV. We confront results of our first-order k_t -factorization calculation against

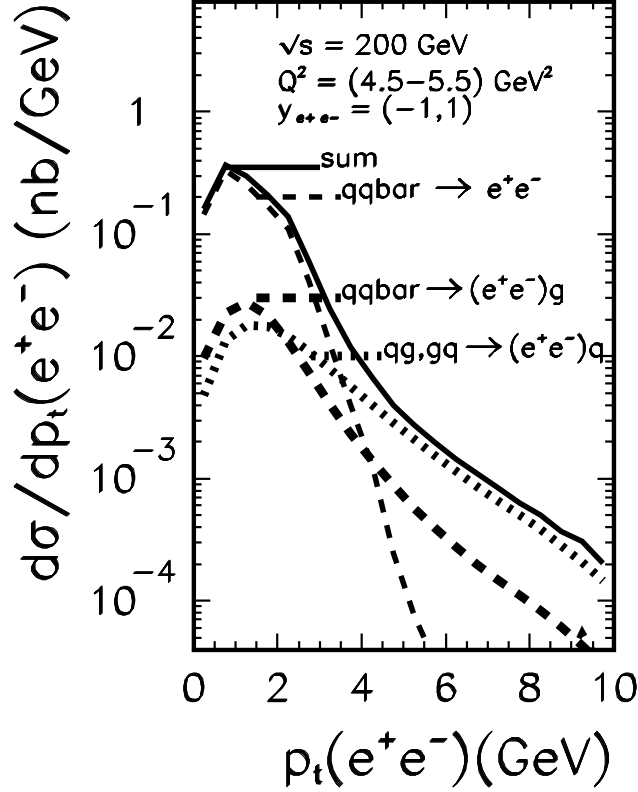


FIG. 12: Distribution in p_{t+} for the RHIC energy $\sqrt{s} = 200$ GeV. We show separately zero-order (dashed line) and first-order Compton (dotted line) contributions. Here $-1 < y(e^+e^-) < 1$ and rapidity of the jet for the first-order contribution is in the full phase space.

UA1 collaboration experimental data [18] which were measured at $p_{t,\mu\mu} > 10$ GeV. We show our results for two different choices of the factorization scale: (a) $\mu_F^2 = M_{\mu\mu}^2$ (left panel), (b) $\mu_F^2 = M_{\mu\mu}^2 + p_{t,\mu\mu}^2$ (right panel). The experimental data are well described within theoretical uncertainties. In this case the zeroth-order contribution (not shown in the figure) is concentrated at $p_{t,\mu\mu} < 10$ GeV.

In the first-order collinear calculations the transverse momentum of the dilepton pair is completely balanced by the transverse momentum of the associated jet (quark or antiquark for the Compton process and gluon for the quark-antiquark annihilation). This strict balance is not longer true when transverse momenta of initial partons are taken into account. In fact the disbalance can be a measure of the transverse momenta of the initial partons. In Fig.17 we show two-dimensional distributions in $(p_{1t}(jet), p_{2t}(e^+e^-))$ for Compton (upper panels) and annihilation (lower panels) contributions for $\sqrt{s} = 200$ GeV and a narrow window in the photon virtuality. We see broad distributions of the strength along diagonal $p_{1t} = p_{2t}$ with a smearing of the order of a few GeV. This smearing is a consequence of the convolution of two unintegrated parton distributions embodied in Eq.(2.4) and (2.5). The broadening

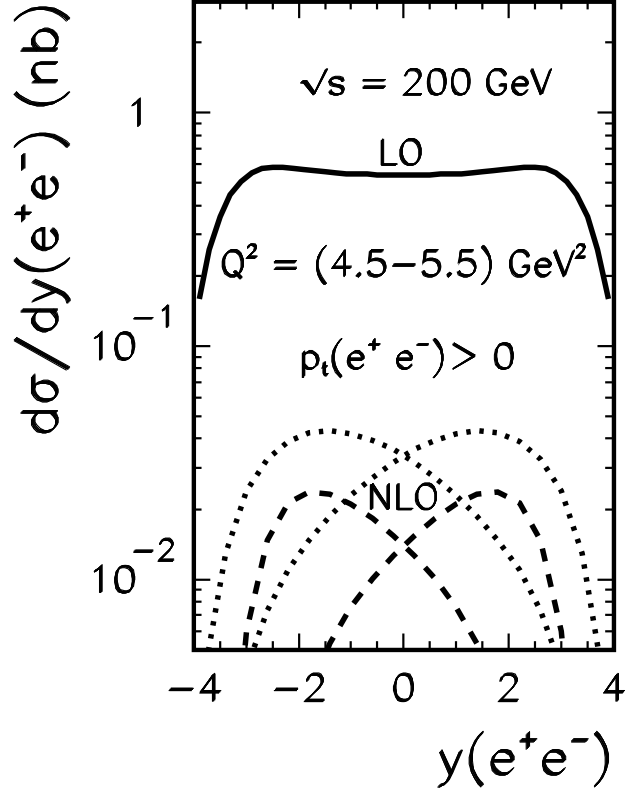


FIG. 13: Distribution in $y(e^+e^-)$ for the RHIC energy $\sqrt{s} = 200$ GeV. We show separately zero-order (solid line) and first-order QCD Compton (dotted line) and quark-antiquark annihilation (dashed line) contributions. The rapidity of the associated jet for the first-order contributions is integrated in the full phase space.

strongly depends on the choice of the factorization scale (compare left and right panels).

In Fig.18 we show similar distributions for the UA1 collaboration experiment. Here the range of transverse momenta of the jet and dilepton pair is much larger. For such a broad range of transverse momenta it looks as if the cross section is concentrated on the diagonal $p_{1t}(jet) = p_{2t}(\mu^+\mu^-)$. A closer inspection shows a smearing similar as shown previously for proton-proton scattering at $\sqrt{s} = 200$ GeV (see Fig.17).

V. CONCLUSIONS

We have calculated both zeroth- and first-order contributions to dilepton production in the formalism with transverse momenta of initial partons taken into account. In these calculations we have used Kwieciński unintegrated parton distributions which include both smearing in parton momentum due to nonperturbative effects in hadrons before collision as well as extra smearing due to QCD evolution effects in the collision process as encoded in

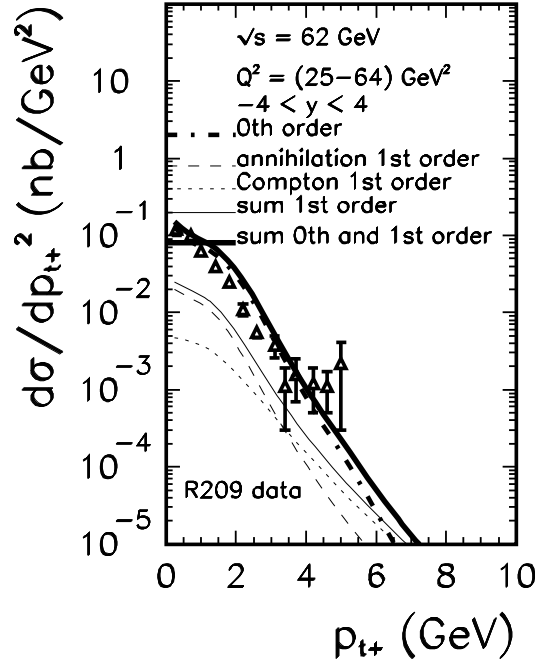


FIG. 14: Distribution in transverse momentum of the dilepton pair in proton-proton collisions. We show both first order contributions: QCD Compton (dotted line) and quark-antiquark annihilation (dashed line). For comparison we show also the zeroth order contribution (dash-dotted line).

the Kwieciński evolution equations.

We have calculated correlations in azimuthal angle between both charged leptons as well as correlations in the two-dimensional space of transverse momentum of the positron and transverse momentum of the electron. Both effect of the Fermi motion and effect of subsequent emissions from the ladder lead to deviations from the delta function in relative azimuthal angle centered at $\phi = \pi$ (collinear case) and deviations from $p_t(\text{electron}) = p_t(\text{positron})$ condition. The shape of the distribution in transverse momentum of the pair depends both on incident energy and virtuality of the time-like photon. This is a straightforward consequence of the QCD evolution encoded in the Kwieciński equations. We predict larger smearing in transverse momentum of the dilepton pair for larger dilepton masses. The existing experimental data at $\sqrt{s} = 62$ GeV can be well explained by the zero-order component by adjusting the parameter responsible for nonperturbative effects of internal motion of partons in hadrons. This is rather in odds with the explanations in the literature, where the data are explained by an extra convolution of the first-order contribution with a Gaussian smearing function. In orthodox collinear the zero-order contribution is completely ignored. The smeared zeroth-order contribution discussed here may be partly responsible for missing strength in the spectrum of so-called nonphotonic electrons [20].

We have also calculated dilepton transverse momentum distribution in the first order for the matrix element. Inclusion of initial transverse momenta removes singularity at $p_{t,l+l-} = 0$. The first-order contribution dominates only at larger transverse momenta of the pair and

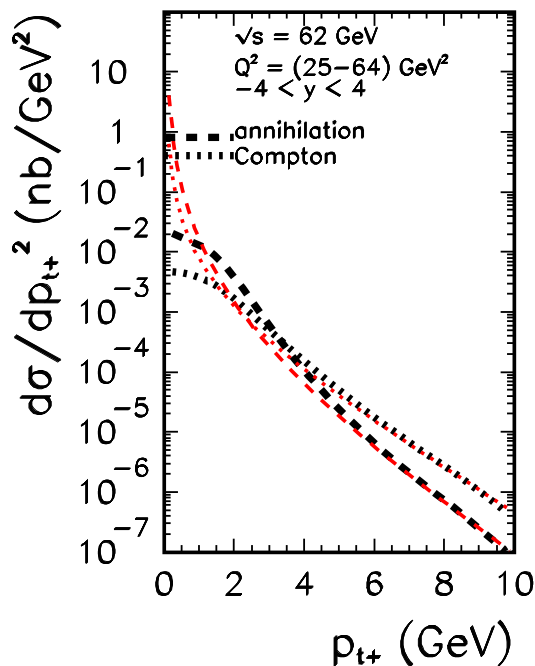


FIG. 15: Distribution in transverse momentum of the dilepton pair for the R209 collaboration experiment. The collinear (thin lines) distributions are compared to k_t -factorization (thick lines) distributions for the QCD Compton (dotted) and quark-antiquark annihilation (dashed).

is smaller than the zeroth-order contribution at low transverse momenta. The inclusion of initial transverse momenta leads naturally to decorrelation of relative azimuthal angle of a jet and dilepton pair (in the first-order collinear approximation they are emitted back-to-back). We have also discussed analogous decorrelations on the $(p_t(jet), p_t(l^+l^-))$ plane. The initial transverse momenta lead to sizeable deviations from the collinear condition $p_t(jet) = p_t(l^+l^-)$.

Finally we wish to make a comment on possible double counting. In principle, our leading order contribution contains diagrams which look like first order diagrams. The standard pQCD first-order result contains large $\log(Q^2/p_t^2)$. For fixed Q^2 it happens when p_t^2 is small. Fortunately it happens numerically that then (in our approach) the first-order result is much lower than the almost purely nonperturbative origin zeroth-order result. In principle, the double counting happens when the zeroth- and first-order results are comparable. As shown in our calculation this happens in a very narrow interval of p_{t+} . So we expect rather small double counting.

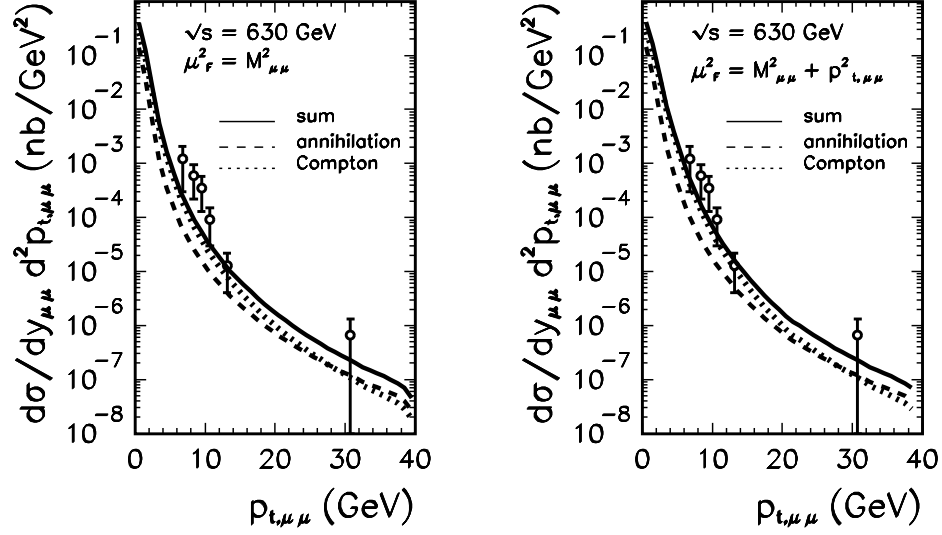


FIG. 16: Dilepton invariant mass distribution for first-order Drell-Yan processes in proton-antiproton scattering for two different scales: $\mu_F^2 = Q^2$ (left panel) and $\mu_F^2 = Q^2 + p_{t, \mu\mu}^2$ (right panel) at $\sqrt{s} = 630$ GeV. Here $Q^2 \in (1, 2.5^2)$ GeV² and $y_2 \in (-1.7, 1.7)$. The contributions of Compton (dotted) and annihilation (dashed) are shown separately. The experimental data of UA1 collaboration are taken from [18].

-
- [1] Ch-Y. Wong and H. Wang, Phys. Rev. **C58** (1998) 376.
 - [2] U. D'Alesio and F. Murgia, Phys. Rev. **D70** (2004) 074009.
 - [3] J. Kwieciński, Acta Phys. Polon. **B33** (2002) 1809. A. Gawron and J. Kwieciński, Acta Phys. Polon. **B34** (2003) 133. A. Gawron, J. Kwieciński and W. Broniowski, Phys. Rev. **D68** (2003) 054001.
 - [4] E. L. Berger, L.E. Gordon and M. Klasen, Phys. Rev. **D58** (1998) 074012.
 - [5] G. Fai, J. Qiu, X. Zhang, Phys. Lett. **B567** (2003) 243.
 - [6] M. Łuszczak and A. Szczurek, Phys. Rev. **D73** (2006) 054028.
 - [7] A. Szczurek, A. Rybarska and G. Ślipek, Phys. Rev. **D76** (2007) 034001.
 - [8] T. Pietrycki and A. Szczurek, Phys. Rev. **D76** (2007) 034003.
 - [9] X.-N. Wang, Phys. Rev. **C61** (2000) 064910.
 - [10] B. Badełek and J. Kwieciński, Phys. Lett. **B295** (1992) 263;
B. Badełek and J. Kwieciński, Rev. Mod. Phys. **68** (1995) 445.
 - [11] A. Szczurek and V. Uleshchenko, Eur. Phys. J. **C12** (2000) 663;
A. Szczurek and V. Uleshchenko, Phys. Lett. **B475** (2000) 120.
 - [12] M. Glück, E. Reya and A. Vogt, Eur.Phys.J. **C5** (1998) 461.
 - [13] J.C. Collins, D.E. Soper and G. Sterman, Nucl. Phys. **B250** (1985) 199.
 - [14] C.T.H. Davies and W.J. Stirling, Nucl. Phys. **B244** (1992) 337.
 - [15] G.A. Ladinsky and C.-P. Yuan, Phys. Rev. **D50** (1994) R4239.

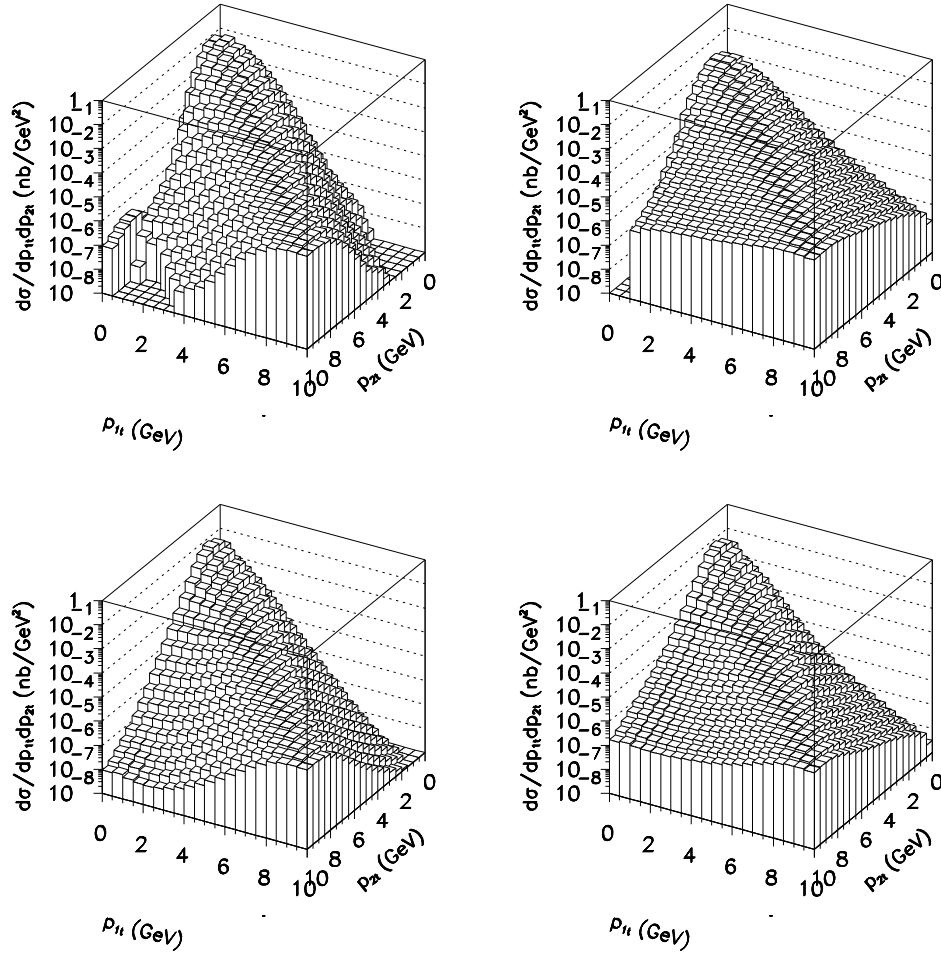


FIG. 17: Two-dimensional distributions in $p_{1t}(jet)$ and $p_{2t}(e^+e^-)$ for the first-order Compton contributions (upper panels) and for the first-order quark-antiquark annihilation contributions (lower panels) in proton-proton collisions at $\sqrt{s} = 200$ GeV and $Q^2 \in (4.5, 5.5)$ GeV². Left panels are for $\mu_F^2 = Q^2$ and right panels for $\mu_F^2 = Q^2 + p_{t,ee}^2$. No cuts on rapidity of the jet as well on the rapidity of the dilepton pair were applied.

- [16] J. Kwieciński and A. Szczurek, Nucl. Phys. **B680** (2003) 164.
- [17] D. Antreasyan et al. (R209 collaboration), Phys. Rev. Lett. **48** (1982) 302.
- [18] C. Albajar et al. (UA1 collaboration), Phys. Lett. **B209** (1988) 397.
- [19] R.D. Field, "Application of Perturbative QCD", Addison-Wesley Publishing Company, Redwood City, 1989.
- [20] M. Łuszczak, R. Maciuła and A. Szczurek, arXiv:0807.5044 [hep-ph].

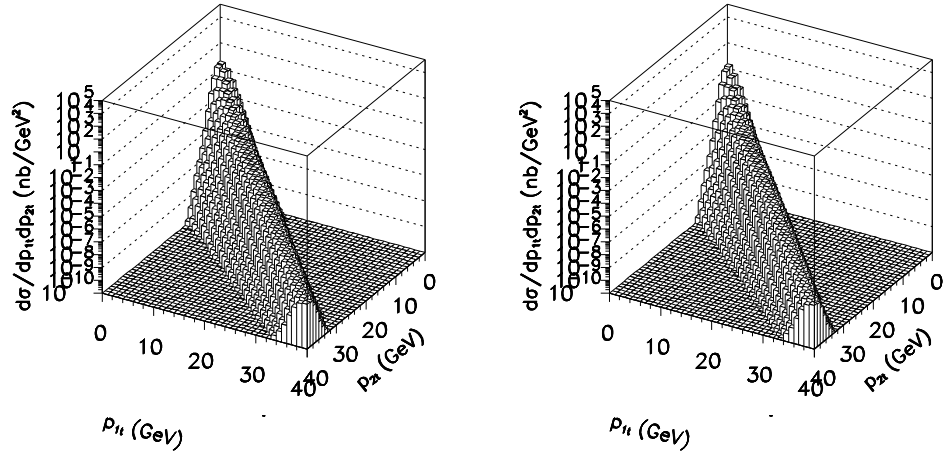


FIG. 18: $(p_{1t}(jet), p_{2t}(\mu\mu))$ distribution for first-order Drell-Yan processes in proton-antiproton collisions at $\sqrt{s} = 630$ GeV. Left panel for QCD Compton and the right panel for annihilation. Here $\mu_F^2 = Q^2$ and $Q^2 = (1, 2.5^2)$ GeV² and $-1.7 < y(\mu^+\mu^-) < 1.7$.